

Anionic hexadeca-carboxylate tetrapyrazinoporphyrazine: synthesis
and *in vitro* photodynamic studies of a water-soluble, non-aggregating
photosensitizer

Miloslav Machacek,^a Jan Kollár,^b Miroslav Miletin,^b Radim Kučera,^b Pavel Kubát,^c Tomas
Simunek,^a Veronika Novakova^{d,*} and Petr Zimcik^{b,*}

^a*Department of Biochemical Sciences, Faculty of Pharmacy in Hradec Kralove, Charles University in Prague,
Heyrovskeho 1203, 500 05, Hradec Kralove, Czech Republic.*

^b*Department of Pharmaceutical Chemistry and Pharmaceutical Analysis, Faculty of Pharmacy in Hradec
Kralove, Charles University in Prague, Heyrovskeho 1203, 500 05, Hradec Kralove, Czech Republic.*

zimcik@faf.cuni.cz, +420 495067257

^c*J. Heyrovský Institute of Physical Chemistry, v.v.i., Academy of Sciences of the Czech Republic, Dolejškova 3,
182 23 Praha 8, Czech Republic.*

^d*Department of Biophysics and Physical Chemistry, Faculty of Pharmacy in Hradec Kralove, Charles University
in Prague, Heyrovskeho 1203, 500 05, Hradec Kralove, Czech Republic. veronika.novakova@faf.cuni.cz, +420
495067380*

Electronic Supplementary Information

Content

| | |
|--|-----|
| Synthesis..... | S3 |
| Preparation of triethyl benzene-1,3,5-tricarboxylate (3)..... | S3 |
| Preparation of 3,5-bis(ethoxycarbonyl)benzoic acid (4)..... | S3 |
| Preparation of diethyl 5-(hydroxymethyl)isophthalate (5)..... | S3 |
| Preparation of diethyl 5-formylisophthalate (6)..... | S3 |
| Characterization..... | S5 |
| NMR spectra..... | S5 |
| Mass spectra | S13 |
| Chromatograms | S14 |
| Detection of singlet oxygen in water..... | S15 |
| Absorption and fluorescence spectra..... | S16 |
| Literature data on photodynamic activity of phthalocyanines..... | S19 |
| Fluorescence microscopy | S20 |
| Experiments with pH inside the cells | S21 |
| Interaction of BSA with 1 | S22 |
| <i>In vitro</i> photodynamic activity | S22 |
| References | S22 |

Synthesis

Preparation of triethyl benzene-1,3,5-tricarboxylate (**3**).

A reported procedure has been adopted for synthesis of this compound.¹ Trimesic acid (20 g, 95 mmol) was dissolved in hot absolute ethanol (145 mL) and sulfuric acid (3.2 mL) was added after dissolution. The mixture was refluxed for 1.5 h and then the condenser was replaced for descending one and about 80 mL of ethanol was distilled off. The reflux then continued for next 3.5 h with appearance of white solid after 1.5 h. The reaction was cooled down and neutralized by saturated NaHCO₃ solution. The white precipitate was collected by filtration and washed by water to yield white solid (23.9 g, 85%) of sufficient purity for next reactions. The analytical sample was crystallized from ethanol. m.p. 132.2-133.1 °C (lit.¹ 136 °C); ¹H NMR (CDCl₃, 500 MHz): δ 8.84 (3H, s), 4.43 (6H, q, *J* = 7.1 Hz), 1.42 (9H, t, *J* = 7.1 Hz); ¹³C NMR (CDCl₃, 125 MHz): δ 165.0, 134.4, 131.4, 61.7, 14.3. Data corresponded well to those published by Kathiresan et al.¹

Preparation of 3,5-bis(ethoxycarbonyl)benzoic acid (**4**).

A reported procedure has been adopted for synthesis of this compound.² The triester **3** (36.1 g, 123 mmol) was dissolved in hot THF (75 mL) and absolute ethanol (120 mL) was added together with finely ground KOH (8.9 g, 135 mmol, contains 85% of the material). The mixture was refluxed for 24 h, cooled down and the volatiles were removed under reduced pressure. Distilled water (450 mL) was added to the remaining solid and the mixture was washed three times with dichloromethane. The organic phase was dried with Na₂SO₄ and evaporated under reduced pressure to recover unreacted triester **3** (6.3 g, 17%). The water phase was acidified with HCl and the white precipitate that formed was collected by filtration and washed with water. The white solid (19.6 g, 60%) contained the product **4** with the traces of 5-(ethoxycarbonyl)isophthalic acid and was of sufficient purity for next reactions. The analytical sample was crystallized from ethanol. m.p. 150.0-150.9 °C (lit.² 153-154 °C); ¹H NMR (CDCl₃, 300 MHz): δ 10.94 (1H, bs), 8.98-8.84 (3H, m), 4.45 (4H, q, *J* = 7.1 Hz), 1.44 (6H, t, *J* = 7.1 Hz); ¹³C NMR (CDCl₃, 75 MHz): δ 170.4, 164.8, 135.4, 135.0, 131.7, 130.2, 61.8, 14.3. Data corresponded well to those published by Leon et al.²

Preparation of diethyl 5-(hydroxymethyl)isophthalate (**5**).

A reported procedure has been adopted for synthesis of this compound.¹ The monocarboxy derivate **4** (17.6 g, 66.1 mmol) was dissolved in anhydrous THF (100 mL) under argon. While cooling the flask by ice water, the 1M solution of BH₃.THF (100 mL, 100 mmol) was added by dropping funnel over a period of 1 h under intense stirring and the white precipitate formed. After all BH₃.THF was added, the reaction was stirred at rt for another 5 h. The reaction was quenched by THF/water 1:1 (150 mL) that was added in a dropwise manner while the reaction flask was cooled by ice water. THF was removed under reduced pressure and the residual water was washed three times with ethyl acetate. Organic layer was dried with Na₂SO₄ and evaporated under reduced pressure. The crude product was purified *via* column chromatography on silica with hexane/ethyl acetate (1:1) as the eluent to yield white solid (13.4 g, 79%). The analytical sample was crystallized from ethanol/water. m.p. 82.3-83.1 °C (lit.¹ 82-83 °C); ¹H NMR (CD₃SOCD₃, 300 MHz): δ 8.36-8.27 (1H, m), 8.16-8.09 (2H, m), 5.49 (1H, t, *J* = 5.7 Hz), 4.62 (2H, d, *J* = 5.7 Hz), 4.33 (4H, q, *J* = 7.1 Hz), 1.33 (6H, t, *J* = 7.1 Hz); ¹H NMR (CD₃SOCD₃, 75 MHz): δ 165.2, 144.5, 131.3, 130.5, 128.0, 62.0, 61.3, 14.3. Data corresponded well to those published by Kathiresan et al.¹

Preparation of diethyl 5-formylisophthalate (**6**).

A reported procedure has been adopted for synthesis of this compound.³ The alcohol **5** (13.4 g, 53.1 mmol) was dissolved in anhydrous chloroform stabilized by amylene (120 mL) under argon. The solution was stirred at rt and pyridinium chlorochromate (28.6 g, 132.8 mmol) was added stepwise. The brown-black suspension was stirred further at rt for 4 h. The solution was then gently decanted

from the black slurry and poured into diethylether. The black slurry in the flask was washed several times with diethylether, the solutions were combined and filtered through Celite. The crude product was purified *via* column chromatography on silica with hexane/ethyl acetate (1:1) as the eluent to yield white solid (11.8 g, 89%). m.p. 88.0-88.9 °C (lit.⁴ 90 °C); ¹H NMR (CDCl₃, 300 MHz): δ 10.12 (1H, s), 8.90 (1H, t, *J* = 1.7 Hz), 8.69 (2H, d, *J* = 1.8 Hz), 4.44 (4H, q, *J* = 7.1 Hz), 1.43 (6H, t, *J* = 7.1 Hz); ¹³C NMR (CDCl₃, 300 MHz): δ 190.5, 164.7, 136.7, 135.6, 134.1, 132.1, 61.8, 14.3. NMR data corresponded well to those published by Dy et al.³

Characterization

NMR spectra

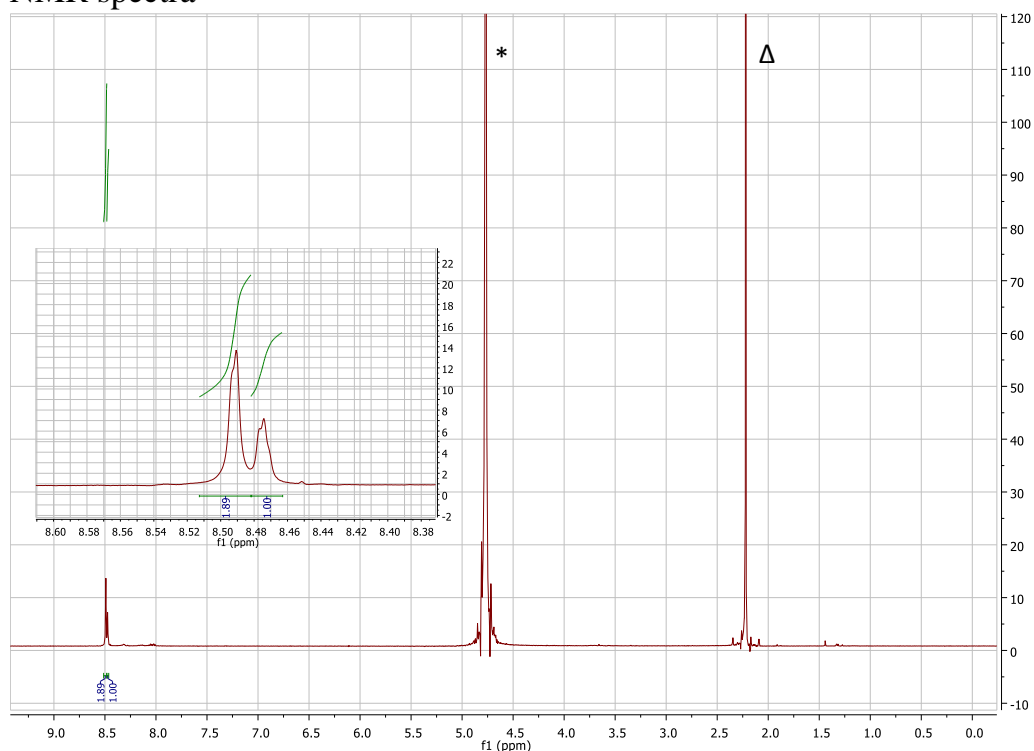


Figure S1. ^1H NMR spectrum (D_2O , 500 MHz) of compound **1**. Asterisk indicates residual signal of non-deuterated solvent, triangle is acetone used to lock the signal.

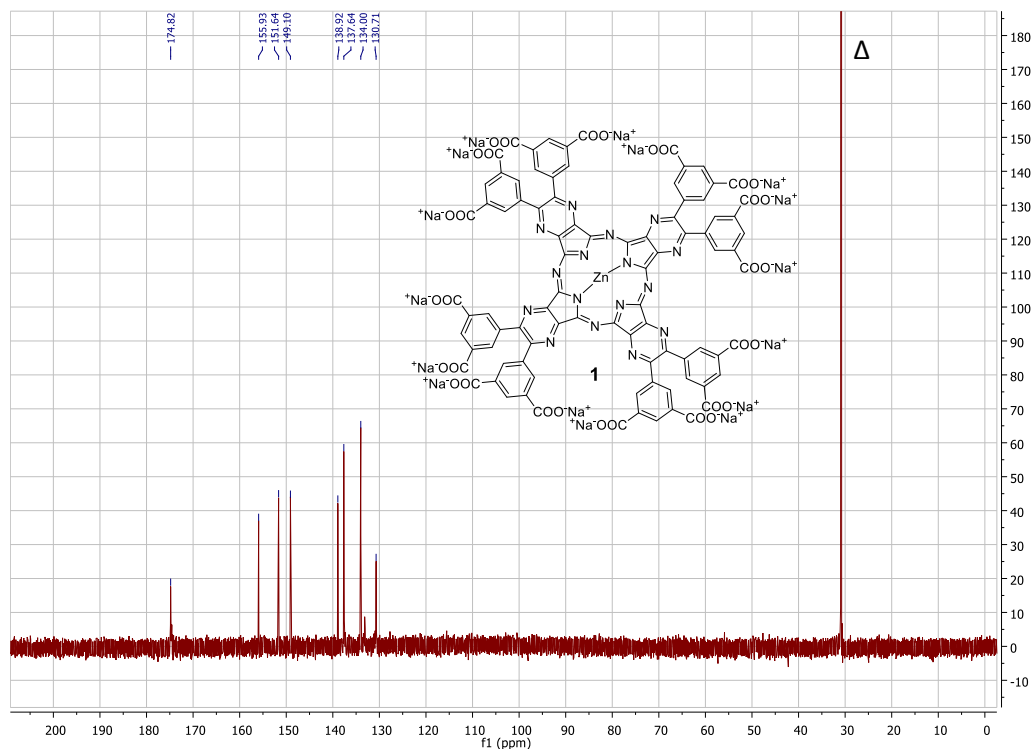


Figure S2. ^{13}C NMR spectrum (D_2O , 125 MHz) of compound **1**. Triangle is acetone used to lock the signal.

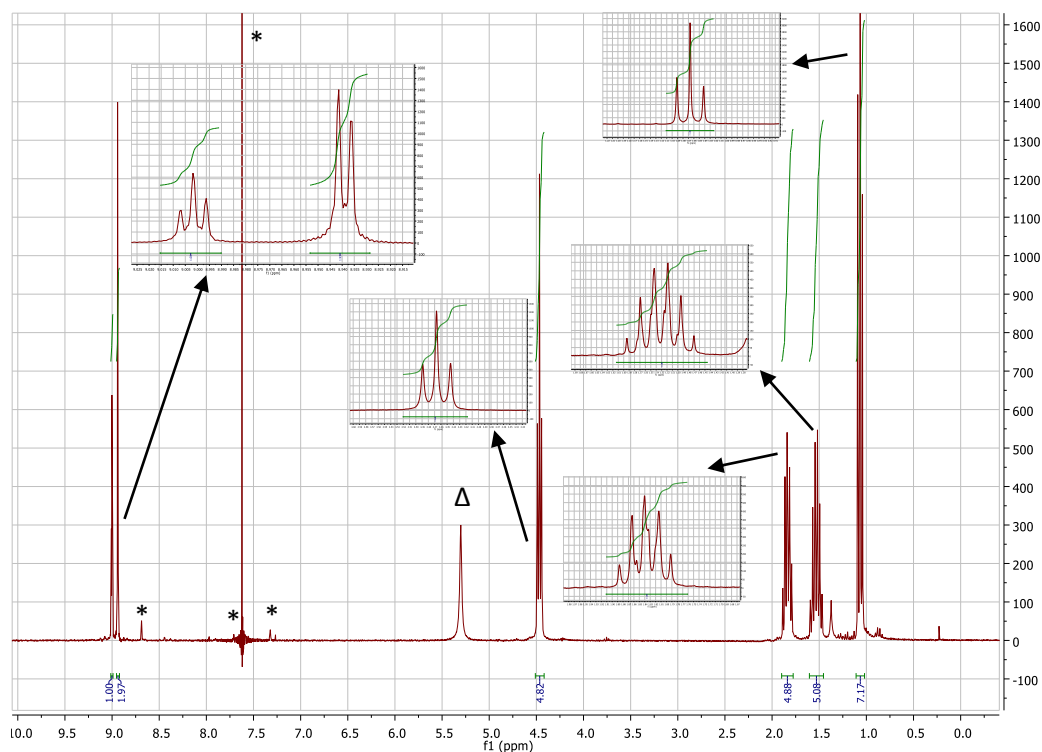


Figure S3. ^1H NMR spectrum ($\text{CDCl}_3/\text{C}_5\text{D}_5\text{N}$ 3:1, 300 MHz) of compound **2Mg**. Asterisks indicate residual signals of non-deuterated solvents, triangle indicates water.

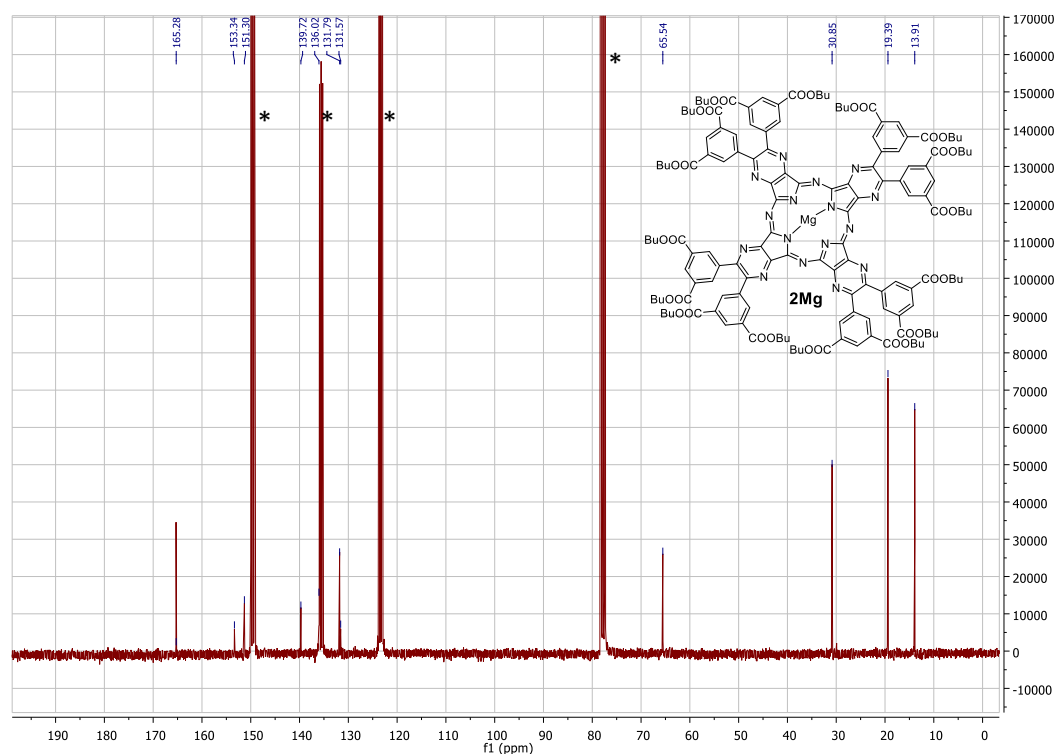


Figure S4. ^{13}C NMR spectrum ($\text{CDCl}_3/\text{C}_5\text{D}_5\text{N}$ 3:1, 75 MHz) of compound **2Mg**. Asterisks indicate signals of solvents.

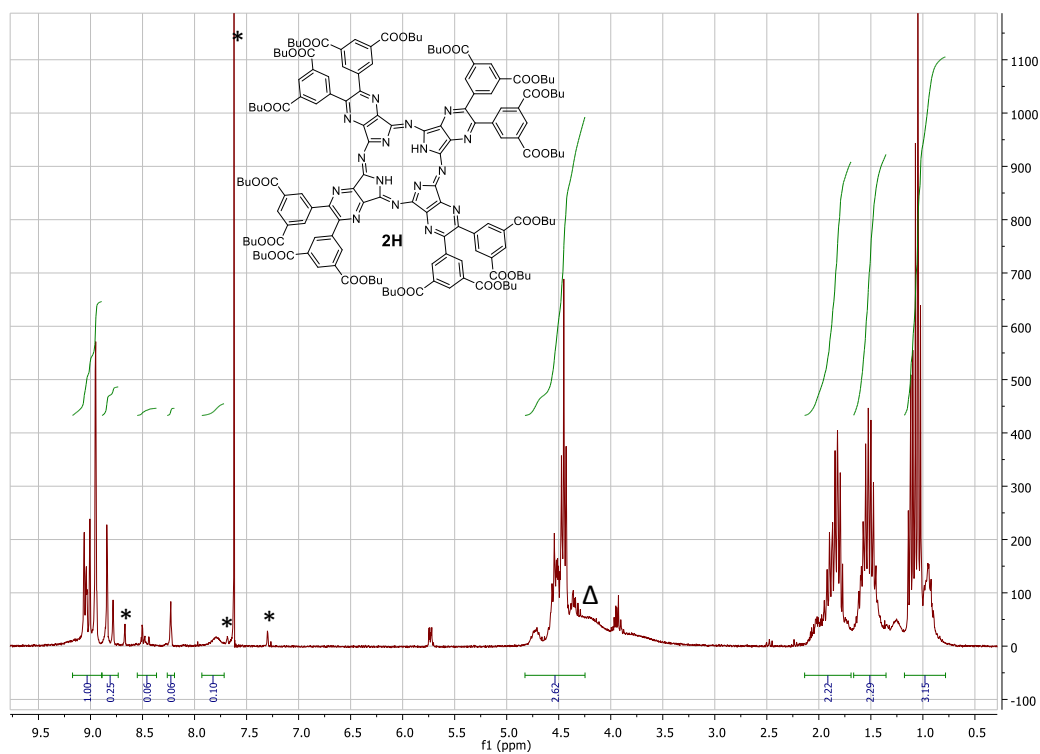


Figure S5. ^1H NMR spectrum ($\text{CDCl}_3/\text{C}_5\text{D}_5\text{N}$ 3:1, 300 MHz) of compound **2H**. Asterisks indicate residual signals of non-deuterated solvents, triangle indicates water.

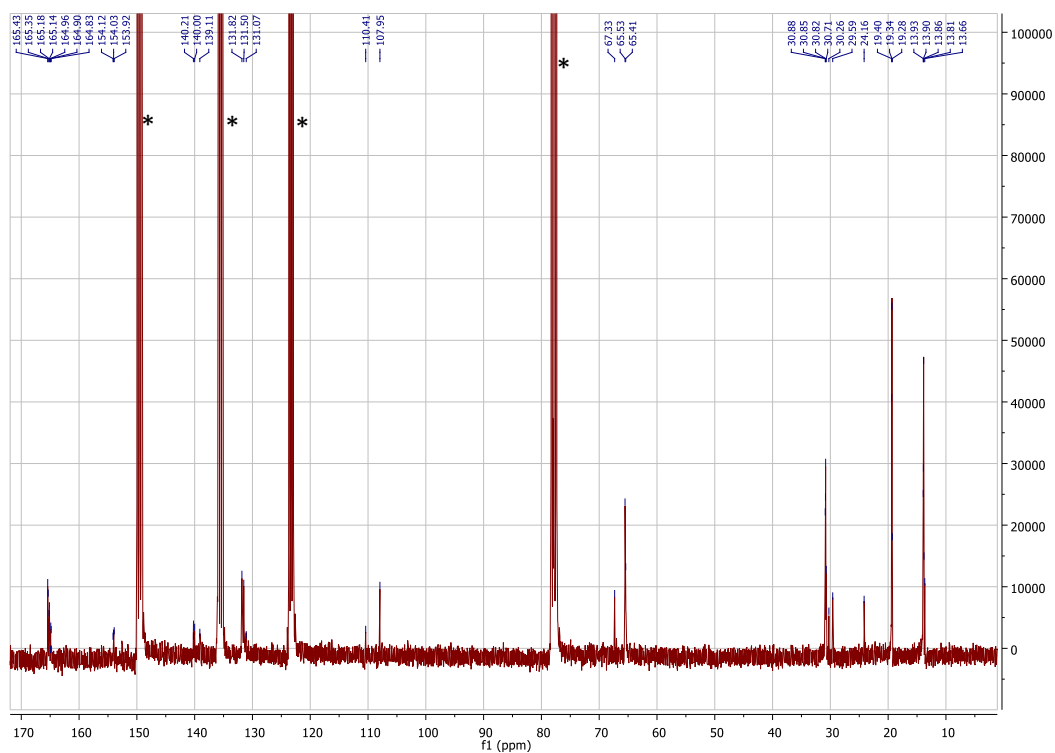


Figure S6. ^{13}C NMR spectrum ($\text{CDCl}_3/\text{C}_5\text{D}_5\text{N}$ 3:1, 75 MHz) of compound **2H**. Asterisks indicate signals of solvents.

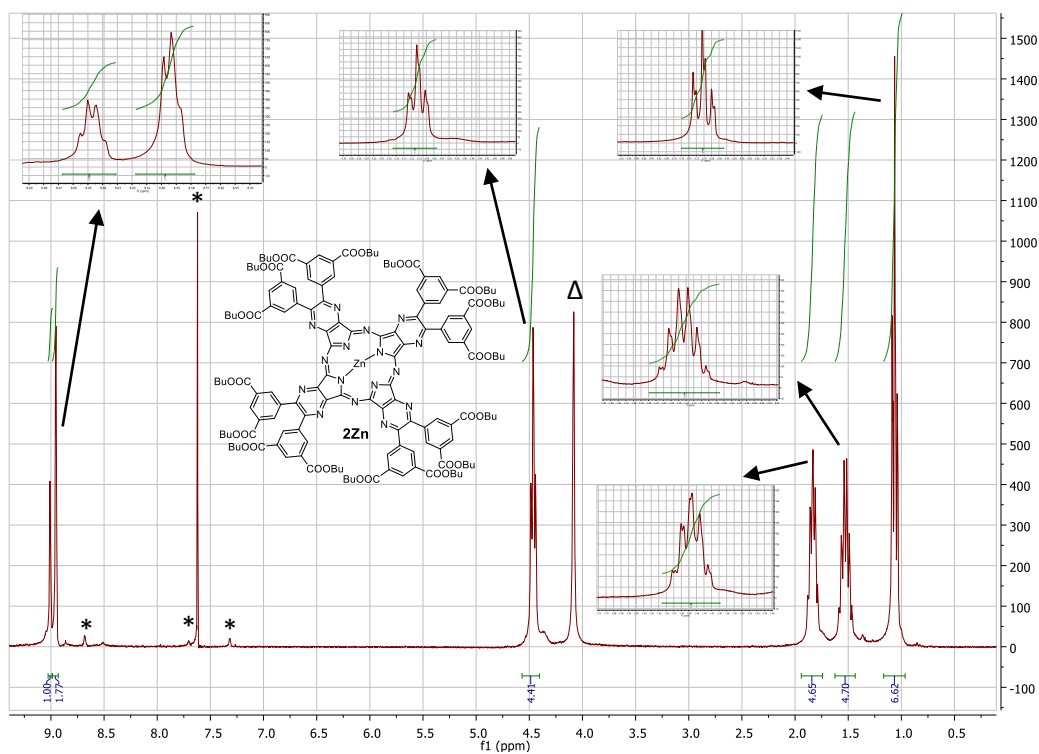


Figure S7. ^1H NMR spectrum ($\text{CDCl}_3/\text{C}_5\text{D}_5\text{N}$ 3:1, 300 MHz) of compound **2Zn**. Asterisks indicate residual signals of non-deuterated solvents, triangle indicates water.

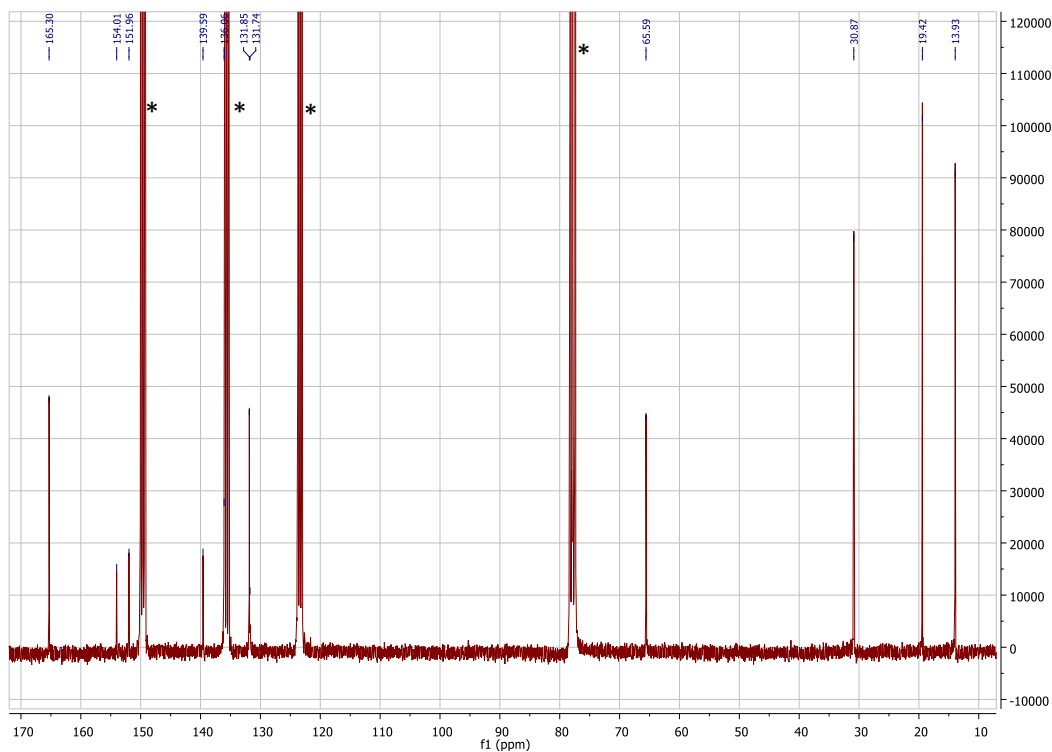


Figure S8. ^{13}C NMR spectrum ($\text{CDCl}_3/\text{C}_5\text{D}_5\text{N}$ 3:1, 75 MHz) of compound **2Zn**. Asterisks indicate signals of solvents.

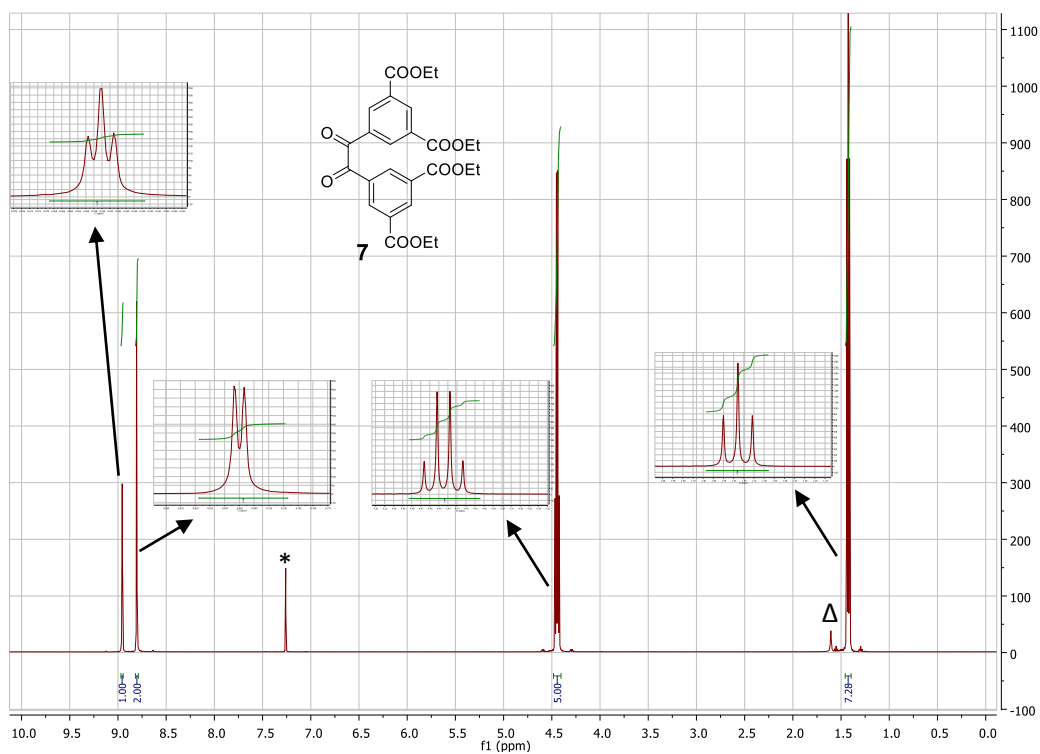


Figure S9. ^1H NMR spectrum (CDCl_3 , 500 MHz) of compound **7**. Asterisk indicates residual signal of non-deuterated solvent, triangle indicates water.

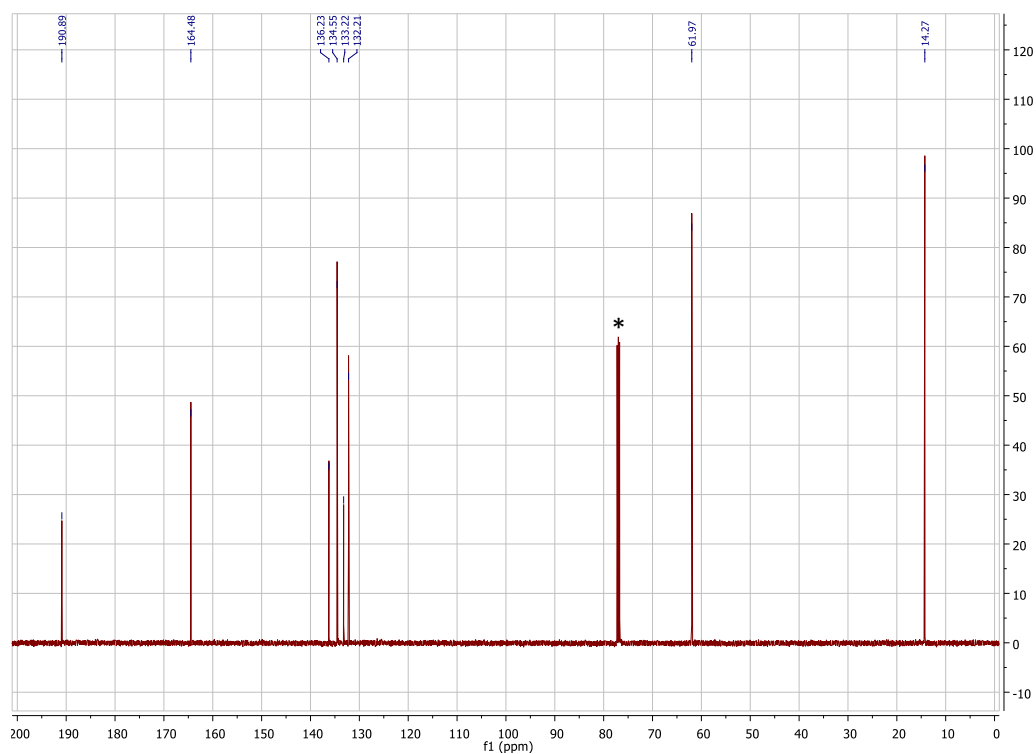


Figure S10. ^{13}C NMR spectrum (CDCl_3 , 125 MHz) of compound **7**. Asterisk indicates signal of solvent.

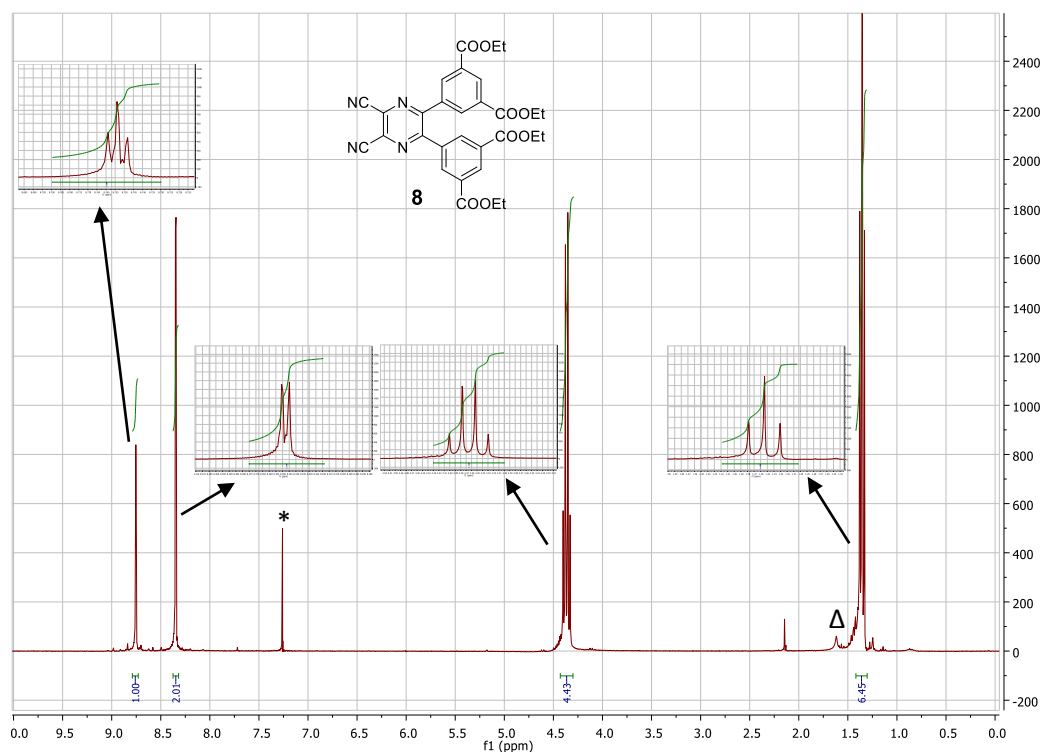


Figure S11. ^1H NMR spectrum (CDCl_3 , 300 MHz) of compound **8**. Asterisk indicates residual signal of non-deuterated solvent, triangle indicates water.

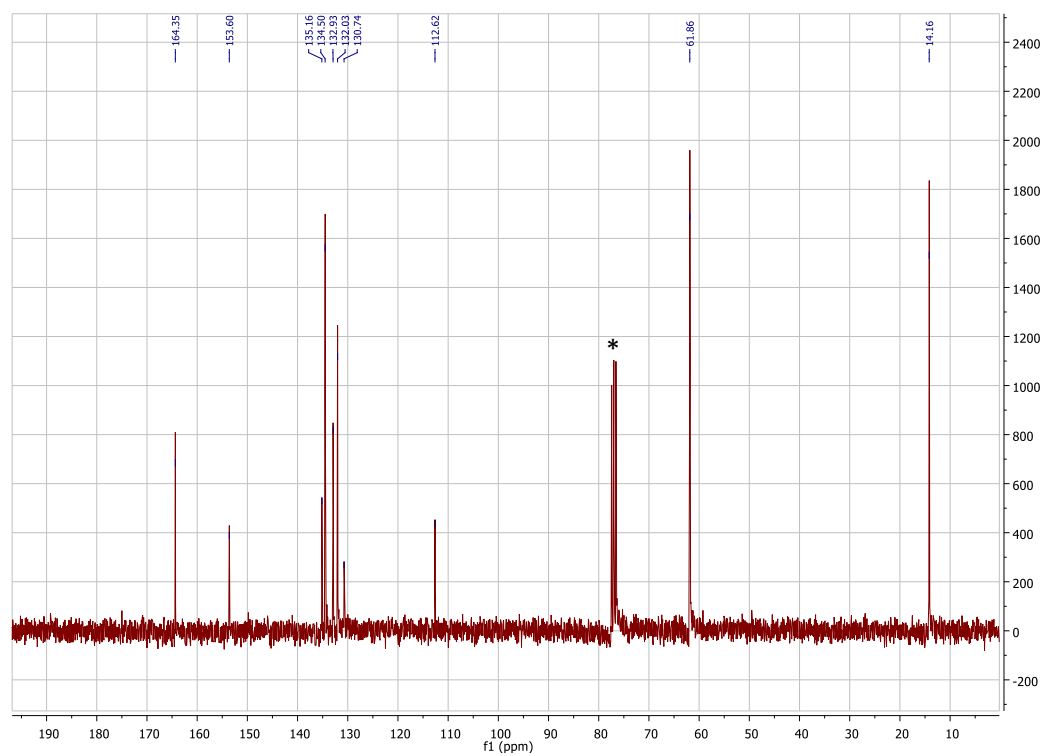


Figure S12. ^{13}C NMR spectrum (CDCl_3 , 75 MHz) of compound **8**. Asterisk indicates signal of solvent.

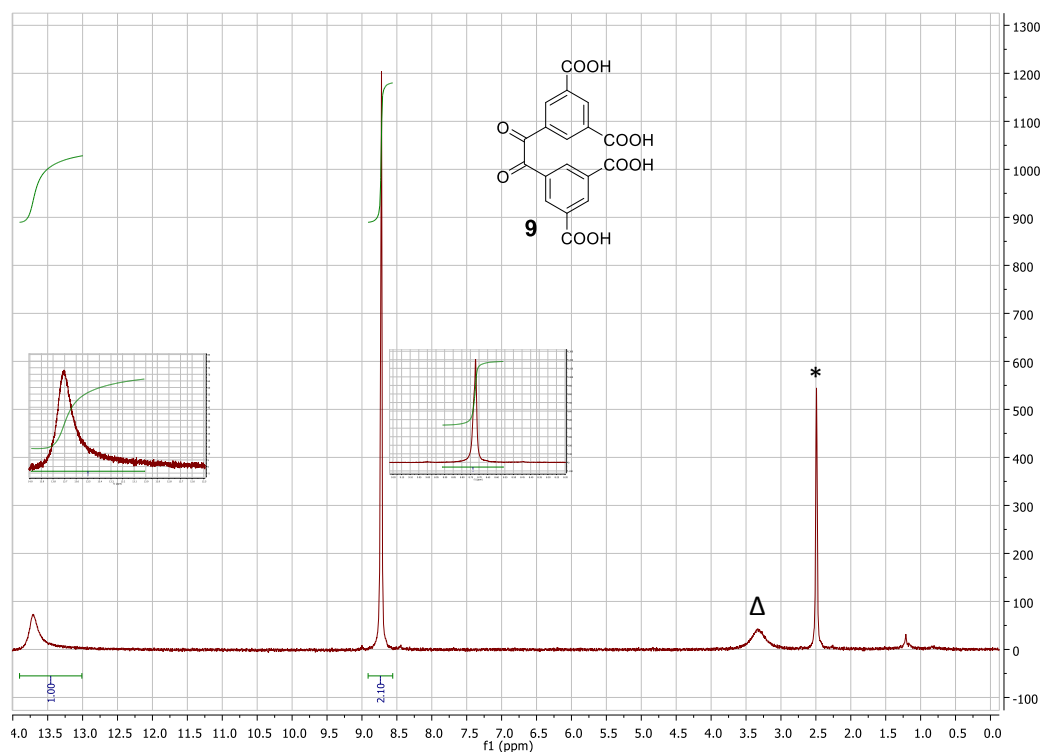


Figure S13. ^1H NMR spectrum (CD_3SOCD_3 , 300 MHz) of compound **9**. Asterisk indicates residual signal of non-deuterated solvent, triangle indicates water.

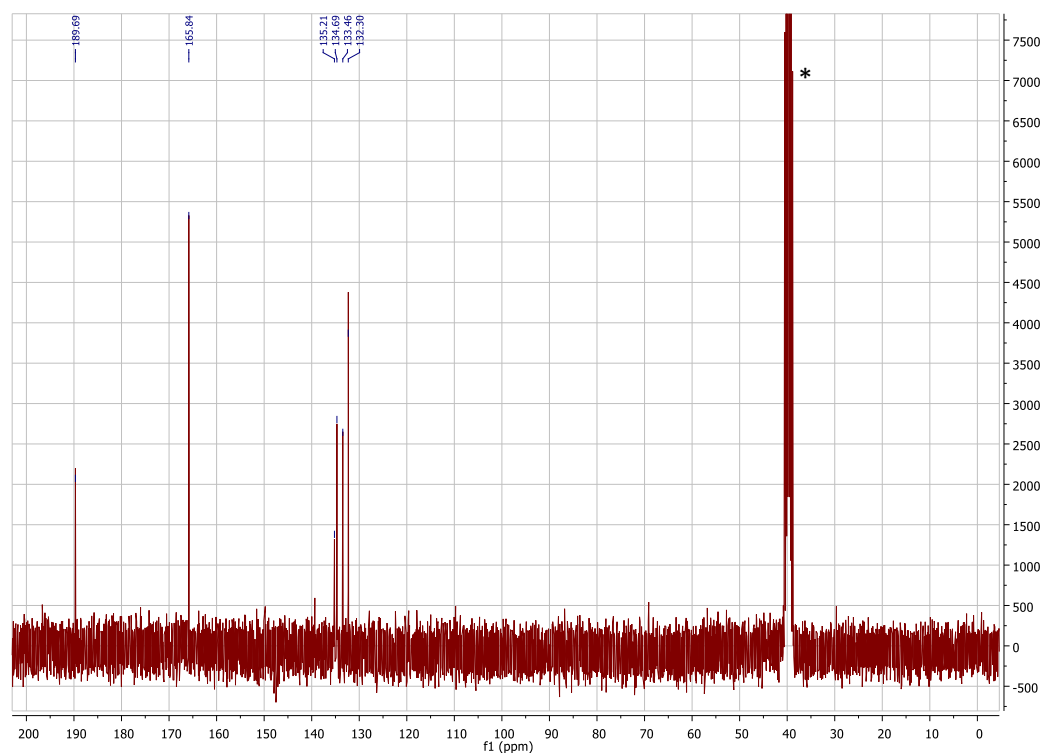


Figure S14. ^{13}C NMR spectrum (CD_3SOCD_3 , 75 MHz) of compound **9**. Asterisk indicates signal of solvent.

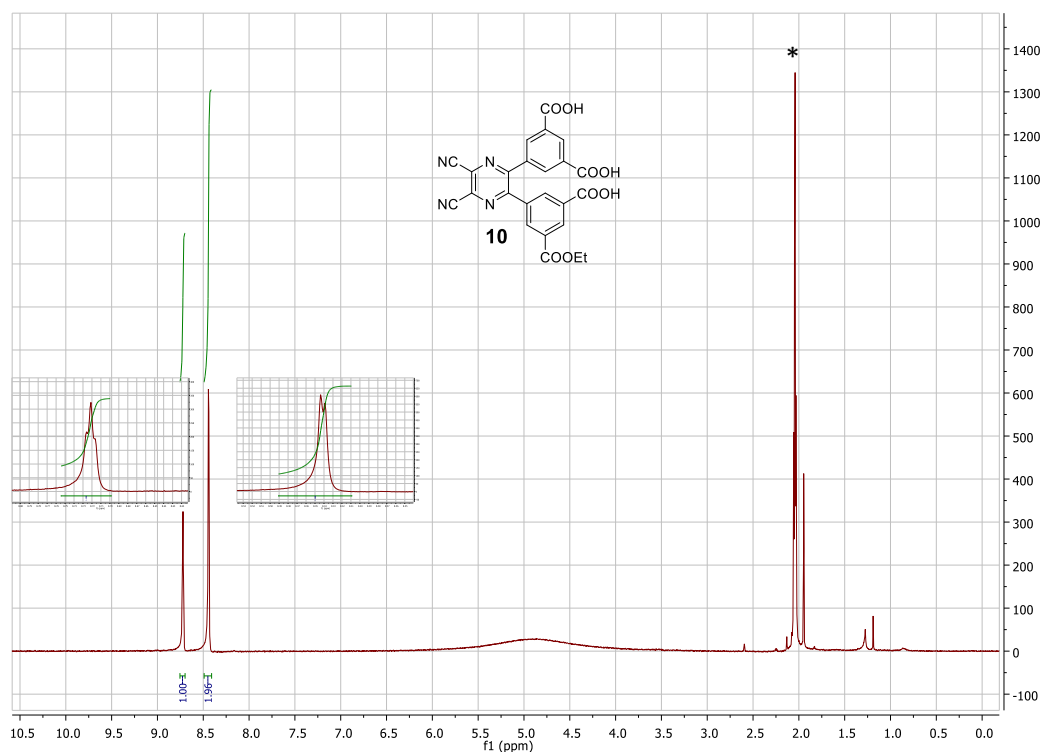


Figure S15. ^1H NMR spectrum (CD_3COCD_3 , 300 MHz) of compound **10**. Asterisk indicates residual signal of non-deuterated solvent.

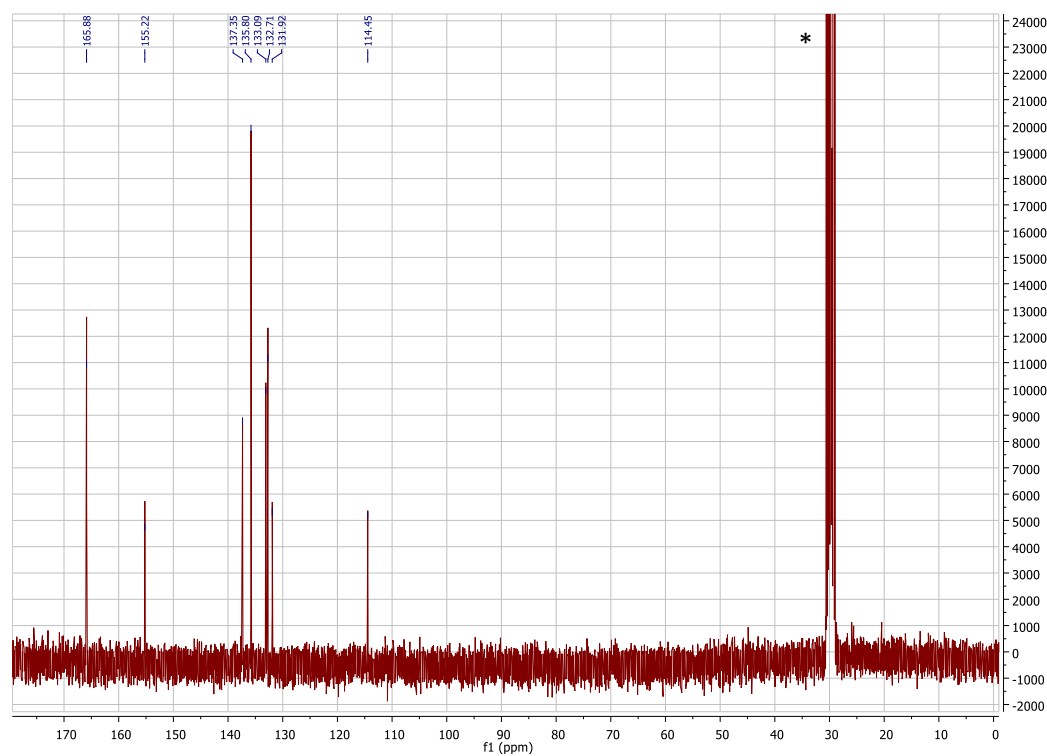


Figure S16. ^{13}C NMR spectrum (CD_3COCD_3 , 75 MHz) of compound **10**. Asterisk indicates signal of solvent.

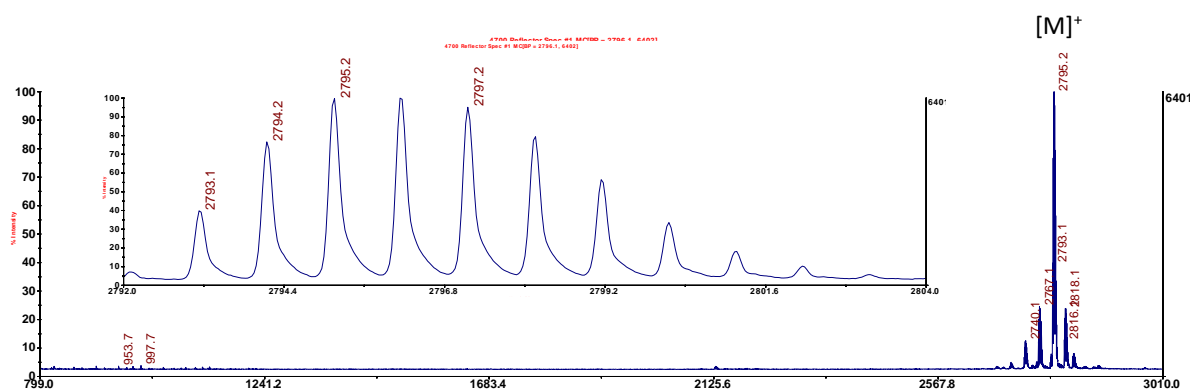


Figure S20. MALDI-TOF mass spectra of compound **2Zn** (positive reflectron mode).

Chromatograms

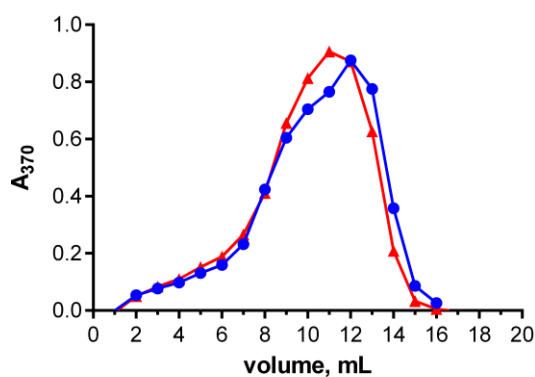


Figure S21. Elution diagram of **1** from gel filtration on Sephadex G-25 monitored as its absorbance at 370 nm after 500 \times dilution of each fraction. Bed diameter: 10 mm. Bed volume: 21 mL. Flow rate 0.3 mL min⁻¹. Two independent experiments (two batches) are shown.

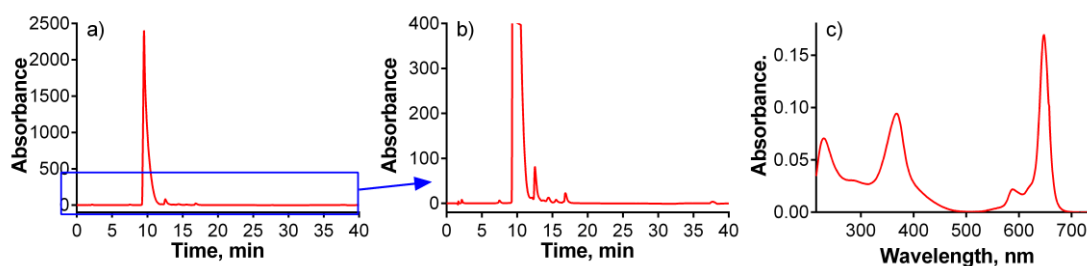


Figure S22. a) HPLC chromatogram of separation of compound **1** (Hypersil BDS C18 column (100 \times 4.6 mm, particle size 2.4 μ m), gradient elution: triethylamine acetate buffer (50 mM, pH 6.3, mobile phase A) and methanol (mobile phase B), λ = 647 nm). b) Enlarged part of the chromatogram. c) Absorption spectrum at t = 9.8 min.

Detection of singlet oxygen in water

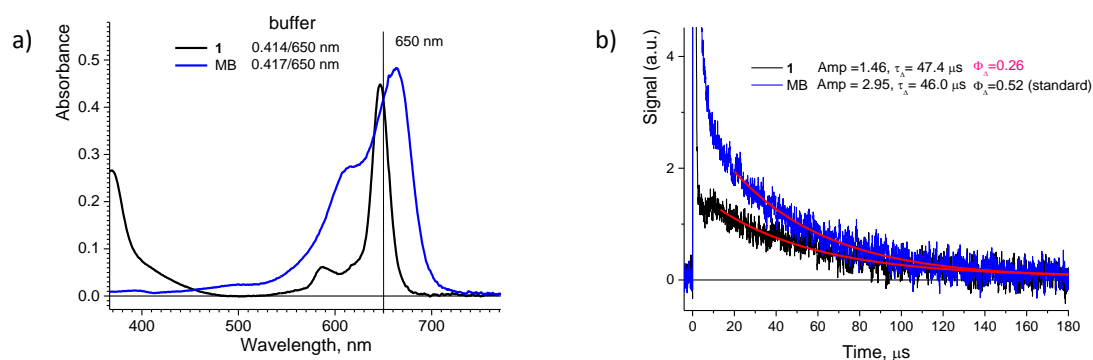


Figure S23. a) Visible spectra of **1** (black) and methylene blue (MB, standard, blue) in D₂O (0.1 M phosphate buffer, pD = 7.1) with absorbances at excitation wavelength ($\lambda_{\text{exc}} = 650$ nm) for calculation of singlet oxygen quantum yield. b) Comparison of singlet oxygen phosphorescence generated from **1** (black) and MB (blue) in D₂O (0.1 M phosphate buffer, pD = 7.1). Excited at 650 nm.

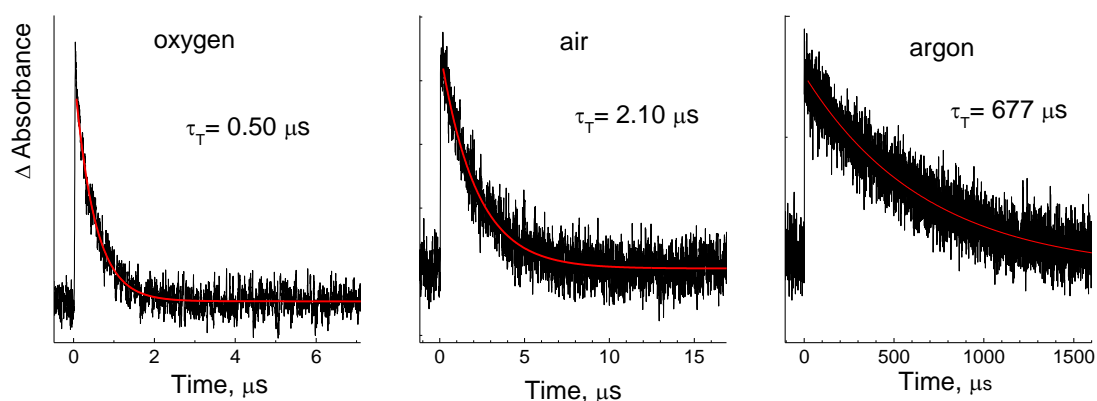


Figure S24. Kinetics of the triplet states of **1** in oxygen-, air-, and argon saturated D₂O monitored at 500 nm. Transient absorption was measured using a LKS 20 laser kinetic spectrometer (Applied Photophysics, UK) equipped with a 150 W Xe lamp, pulse unit and R928 photomultiplier (Hamamatsu) upon laser excitation at 650 nm.

Absorption and fluorescence spectra

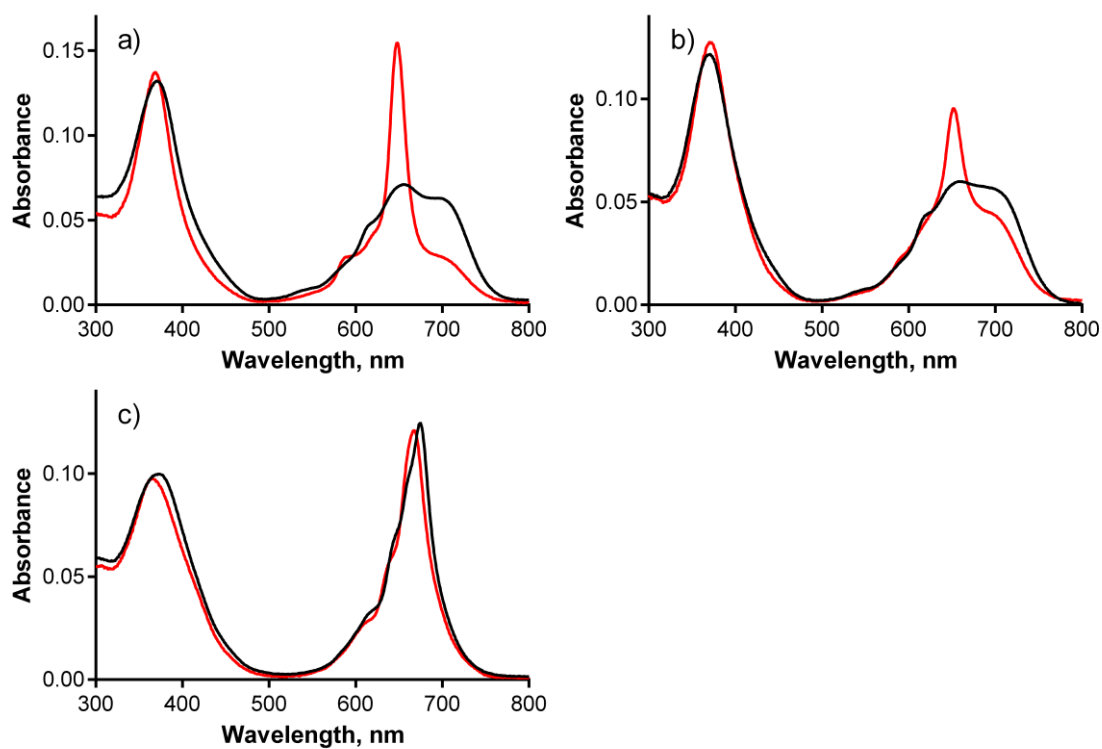


Figure S25. Absorption spectra of **2Zn** (a), **2Mg** (b) and **2H** (c) in THF (red) and toluene (black) at concentrations approximately 1 μM .

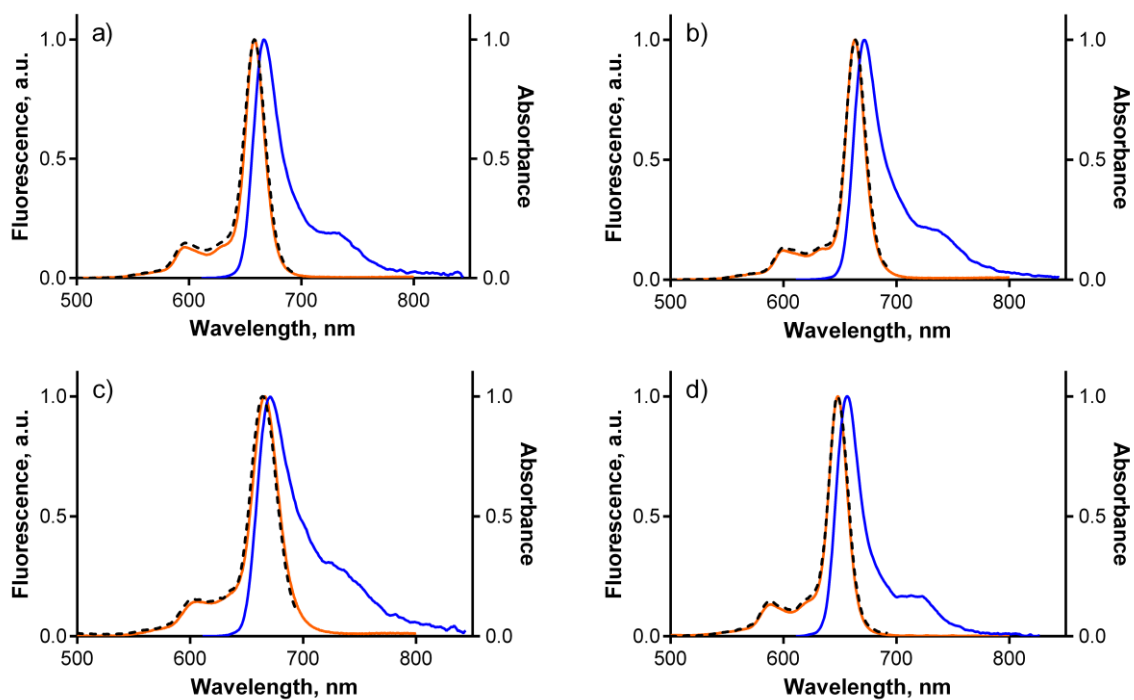


Figure S26. Normalized absorption (orange), emission (blue) and excitation (black dashed) spectra of **2Zn** (a), **2Mg** (b) and **2H** (c) in pyridine and **1** (d) in water.

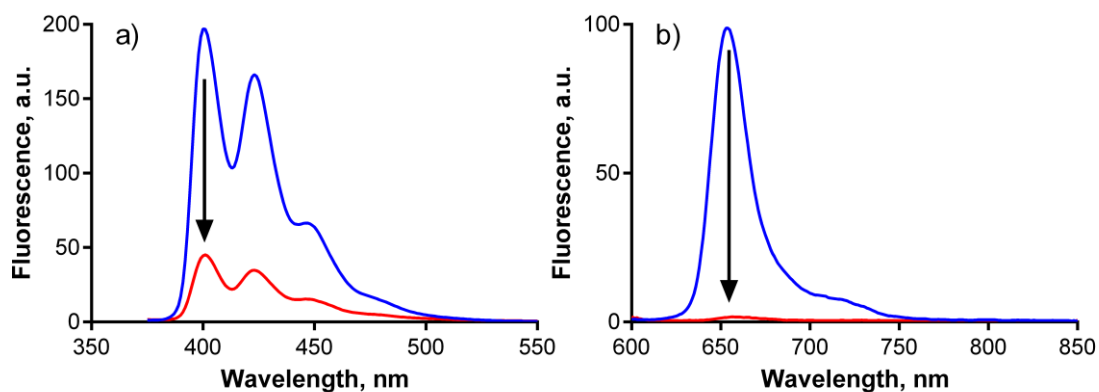


Figure S27. Mutual quenching of the fluorescence of LysoTrackerBlue (a, $\lambda_{\text{exc}} = 354$ nm) and compound **1** (b, $\lambda_{\text{exc}} = 588$ nm) in buffer solution with pH = 5.1. Blue lines - the dye alone (1 μM) in buffer, red lines - after mixing the two dyes (final concentration of each component is 1 μM).

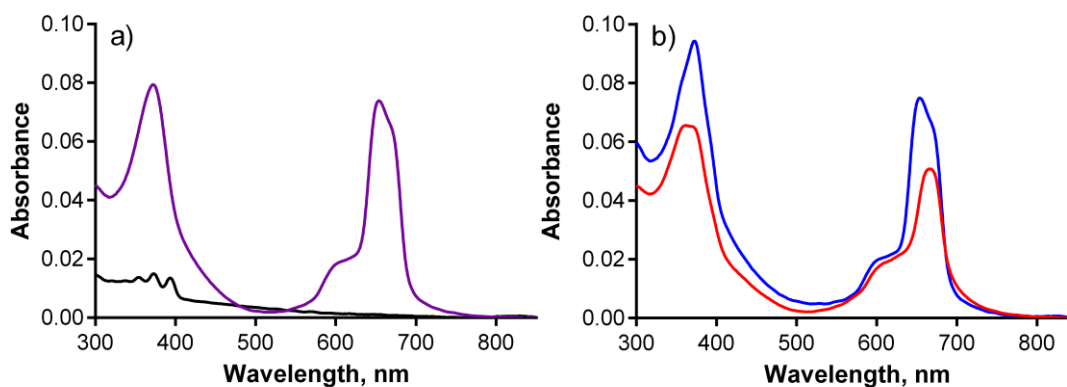


Figure S28. a) Absorption spectra of LysoTrackerBlue (black) and compound **1** (magenta) in buffer solution with pH = 5.1 at concentration of 1 μM . b) Sum (blue) of the absorption spectra of **1** and LysoTrackerBlue in buffer solution with pH = 5.1 at concentration of 1 μM and absorption spectrum of the mixture of these two compounds (red) after mixing the two dyes (final concentration of each component is 1 μM).

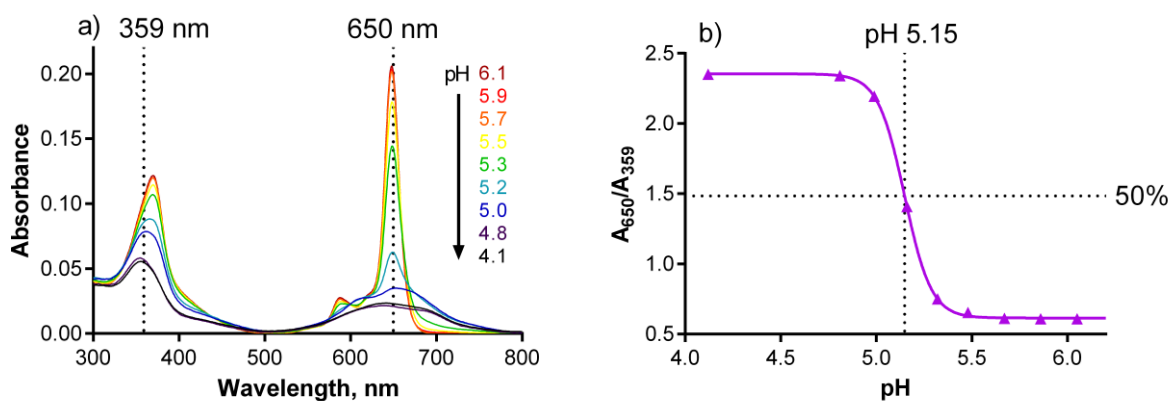
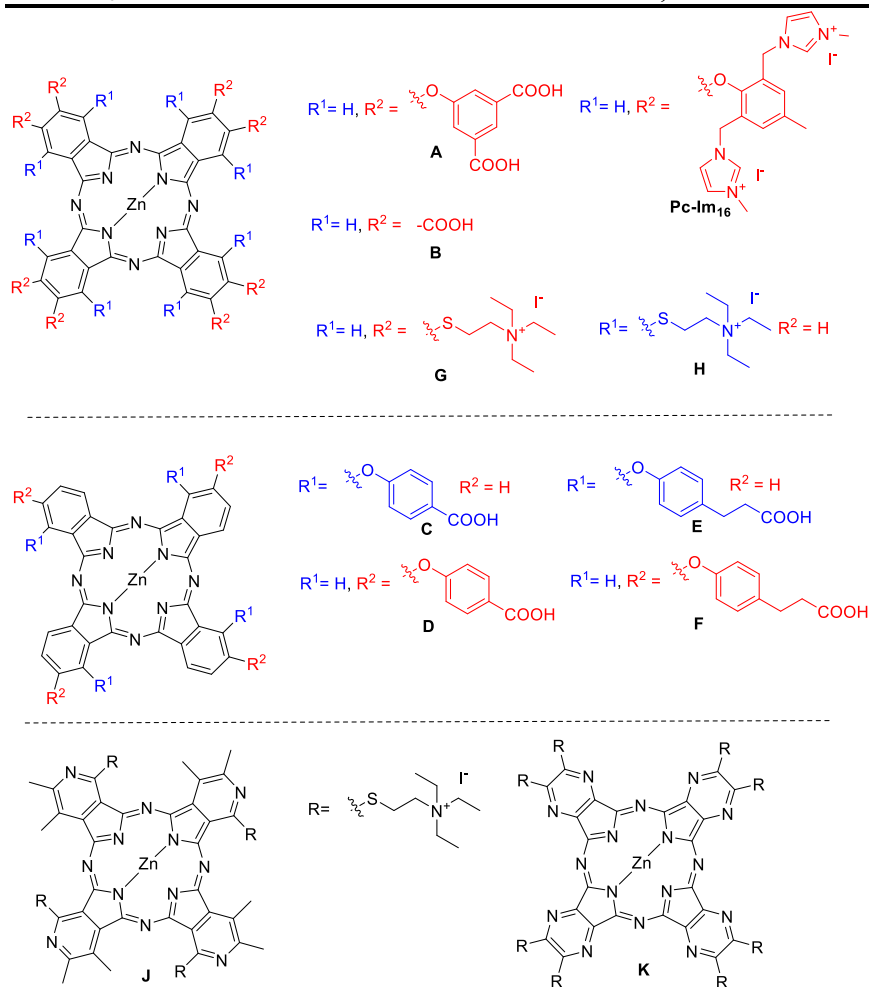


Figure S29. a) Changes in absorption spectra of **1** ($c \sim 1 \mu\text{M}$) in buffer of different pH. b) Dependence of ratio of absorbance at 650 nm and 359 nm of **1** on pH.

Literature data on photodynamic activity of phthalocyanines

Table S1. Photodynamic activity of water soluble anionic and cationic Pcs and aza-analogs.

| Compound | Type | Cells | Irradiation | IC ₅₀ (μM) | Reference |
|---------------------------|----------|-----------|---|-----------------------|-----------|
| 1 | Anionic | HeLa | λ > 570 nm, 11.2 J cm ⁻² | 5.7 | This work |
| A | Anionic | J774 | λ > 600 nm, 48 J cm ⁻² | ~ 1 | 5 |
| A | Anionic | HepG2 | λ > 600 nm, 48 J cm ⁻² | > 4 | 5 |
| A | Anionic | HEp2 | λ > 610 nm, 1 J cm ⁻² | 4.5 | 6 |
| B | Anionic | HeLa | λ > 500 nm, 31 J cm ⁻² | > 10 | 7 |
| C | Anionic | MGC803 | λ > 610 nm, 60 J cm ⁻² | 3.05 | 8 |
| C | Anionic | Bel-7402 | λ = 600-700 nm, 53.7 J cm ⁻² | ~ 18 | 9 |
| D | Anionic | MGC803 | λ > 610 nm, 60 J cm ⁻² | 3.29 | 8 |
| E | Anionic | MGC803 | λ > 610 nm, 60 J cm ⁻² | 3.78 | 8 |
| F | Anionic | MGC803 | λ > 610 nm, 60 J cm ⁻² | 5.30 | 8 |
| G | Cationic | HeLa | λ > 570 nm, 11.2 J cm ⁻² | 0.54 | 10 |
| G | Cationic | SK-MEL-28 | λ > 570 nm, 11.2 J cm ⁻² | 0.32 | 10 |
| H | Cationic | HeLa | λ > 570 nm, 11.2 J cm ⁻² | 0.31 | 10 |
| H | Cationic | SK-MEL-28 | λ > 570 nm, 11.2 J cm ⁻² | 0.22 | 10 |
| J | Cationic | HeLa | λ > 570 nm, 11.2 J cm ⁻² | 0.26 | 11 |
| K | Cationic | HeLa | λ > 570 nm, 11.2 J cm ⁻² | 3.70 | 10 |
| K | Cationic | Hep2 | λ > 640 nm, 52.2 J cm ⁻² | 0.10 | 12 |
| Pc-Im₁₆ | Cationic | HeLa | λ > 570 nm, 11.2 J cm ⁻² | 0.037 | 13 |



Fluorescence microscopy

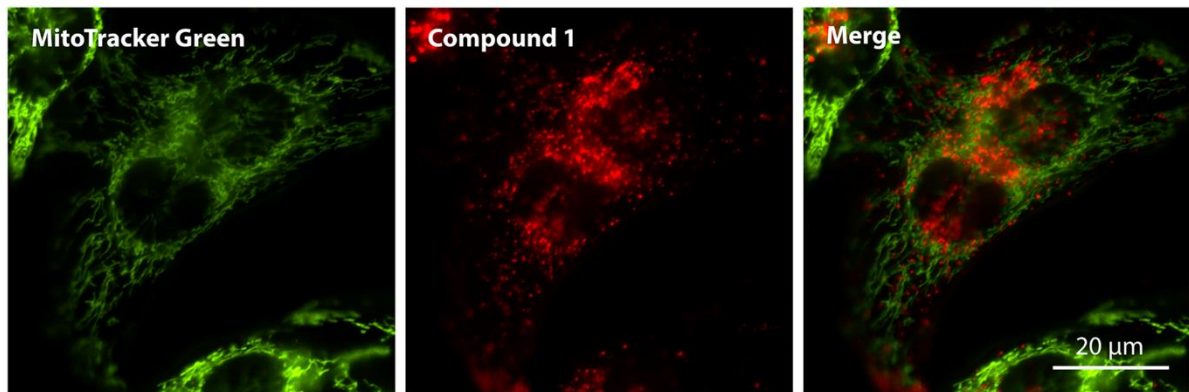


Figure S30. Subcellular localization of compound **1** (red) in HeLa cells visualized by fluorescence microscopy after co-incubation with MitoTracker (green). No co-localization is observed.

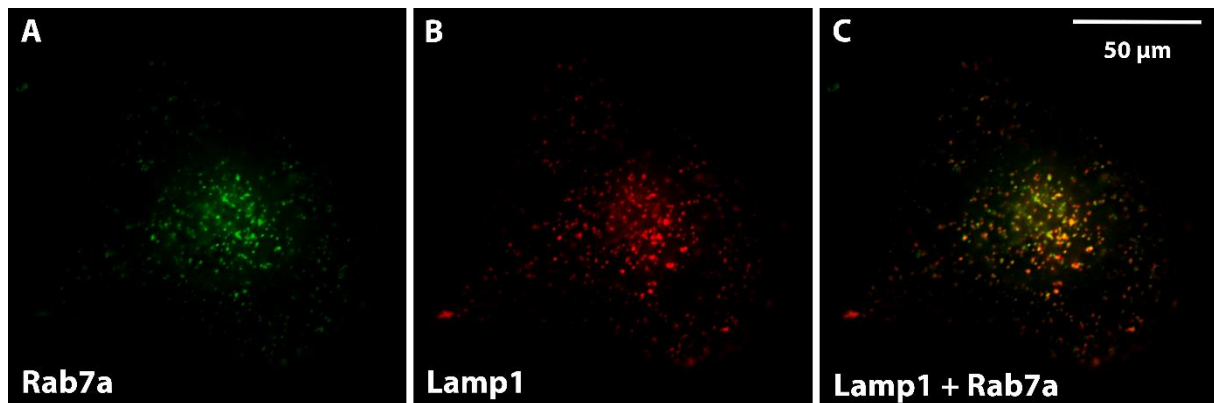


Figure S31. Subcellular localization of Rab7a-GFP (A, green) and Lamp1-RFP (B, red) on endo-lysosomal vesicles in HeLa cells visualized by fluorescence microscopy.

Experiments with pH inside the cells

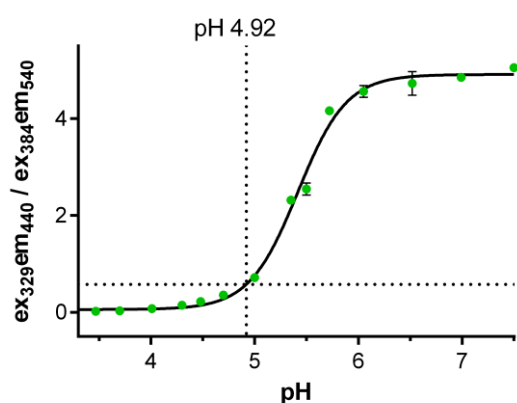


Figure S32. Determination of lysosomal pH using LysoSensor Yellow/Blue DND-160. Green dots are data for calibration curve determined in buffer (made in duplicate), black line is the best fit. The lysosomal pH in HeLa cells was subsequently determined to be 4.9 using the calibration curve.

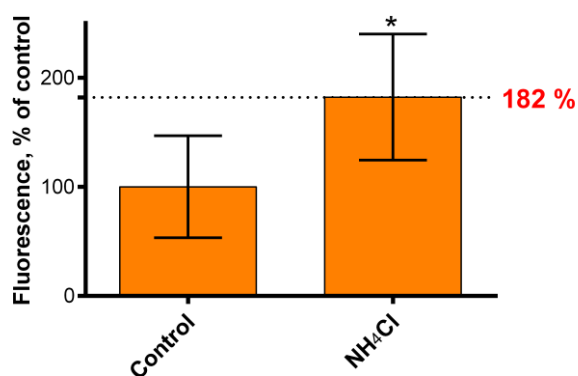


Figure S33. Effect of alkalization of lysosomes in HeLa cells with 20 mM NH₄Cl on fluorescence intensity of **1** ($\lambda_{exc} = 375$ nm, $\lambda_{em} = 671$ nm) monitored by Tecan Infinite M 200 plate reader. Five independent experiments were performed. Cells were seeded on 96-well plates and incubated with **1** for 12 h. Ammonium chloride was added for 15 min prior to fluorescent measurement. Key: *, $p < 0.05$.

Interaction of BSA with **1**

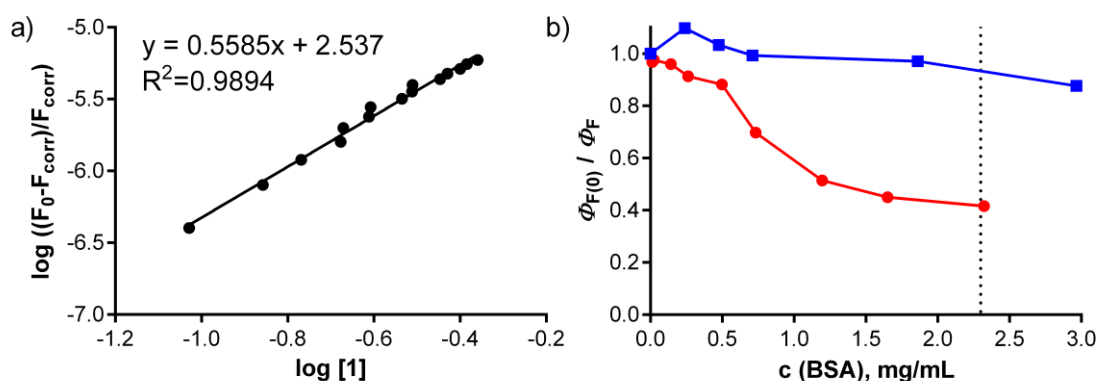


Figure S34. a) Determination of binding constant (K_b) between BSA and compound **1** in SFM. ($c_{(\text{BSA})} = 2 \mu\text{M}$, $\lambda_{\text{exc}}=280 \text{ nm}$, $\lambda_{\text{em}}=340 \text{ nm}$). b) Dependence of normalized Φ_F of **1** (red) and **Pc-Im16** (blue) in SFM on the amount of added BSA. Dotted line indicates the typical amount of BSA in SCM.

In vitro photodynamic activity

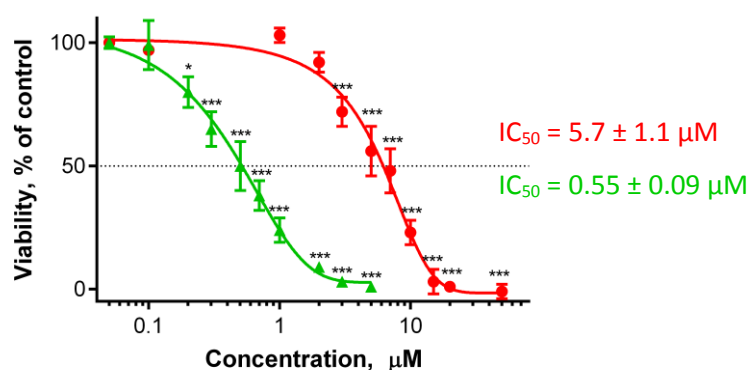


Figure S35. Phototoxicity ($\lambda > 570 \text{ nm}$, 12.4 mW cm^{-2} , 15 min , 11.2 J cm^{-2}) of **1** against the HeLa cells. Compound **1** was applied as a solution in SFM (green, triangle) or in SCM (red, dots). Typically four independent experiments, each in quadruplicate, were performed. Key: *, $p < 0.05$; **, $p < 0.01$; ***, $p < 0.001$.

References

- (1) Kathiresan, M.; Walder, L.; Ye, F.; Reuter, H. Viologen-based benzylic dendrimers: selective synthesis of 3,5-bis(hydroxymethyl) benzylbromide and conformational analysis of the corresponding viologen dendrimer subunit *Tetrahedron Lett.* **2010**, *51*, 2188-2192.
- (2) Leon, J. W.; Kawa, M.; Frechet, J. M. J. Isophthalate ester-terminated dendrimers: Versatile nanoscopic building blocks with readily modifiable surface functionalities *J. Am. Chem. Soc.* **1996**, *118*, 8847-8859.
- (3) Dy, J. T.; Ogawa, K.; Satake, A.; Ishizumi, A.; Kobuke, Y. Water-soluble self-assembled butadiyne-bridged bisporphyrin: A potential two-photon-absorbing photosensitizer for photodynamic therapy *Chem.-Eur. J.* **2007**, *13*, 3491-3500.

- (4) Ashton, P. R.; Fyfe, M. C. T.; Hickingbottom, S. K.; Menzer, S.; Stoddart, J. F.; White, A. J. P.; Williams, D. J. Combining different hydrogen-bonding motifs to self-assemble interwoven superstructures *Chem.-Eur. J.* **1998**, *4*, 577-589.
- (5) Choi, C. F.; Tsang, P. T.; Huang, J. D.; Chan, E. Y. M.; Ko, W. H.; Fong, W. P.; Ng, D. K. P. Synthesis and in vitro photodynamic activity of new hexadeca-carboxy phthalocyanines *Chem. Commun.* **2004**, 2236-2237.
- (6) Liu, W.; Jensen, T. J.; Fronczek, F. R.; Hammer, R. P.; Smith, K. M.; Vicente, M. G. H. Synthesis and Cellular Studies of Nonaggregated Water-Soluble Phthalocyanines *J. Med. Chem.* **2005**, *48*, 1033-1041.
- (7) Oda, K.; Ogura, S.-i.; Okura, I. Preparation of a water-soluble fluorinated zinc phthalocyanine and its effect for photodynamic therapy *J. Photochem. Photobiol., B* **2000**, *59*, 20-25.
- (8) Ke, M.-R.; Huang, J.-D.; Weng, S.-M. Comparison between non-peripherally and peripherally tetra-substituted zinc (II) phthalocyanines as photosensitizers: Synthesis, spectroscopic, photochemical and photobiological properties *J. Photochem. Photobiol., A* **2009**, *201*, 23-31.
- (9) Xia, C.; Wang, Y.; Chen, W.; Yu, W.; Wang, B.; Li, T. New Hydrophilic/Lipophilic Tetra- α -(4-carboxyphenoxy) Phthalocyanine Zinc-Mediated Photodynamic Therapy Inhibits the Proliferation of Human Hepatocellular Carcinoma Bel-7402 Cells by Triggering Apoptosis and Arresting Cell Cycle *Molecules* **2011**, *16*, 1389.
- (10) Machacek, M.; Cidlina, A.; Novakova, V.; Svec, J.; Rudolf, E.; Miletin, M.; Kučera, R.; Simunek, T.; Zimcik, P. Far-Red-Absorbing Cationic Phthalocyanine Photosensitizers: Synthesis and Evaluation of the Photodynamic Anticancer Activity and the Mode of Cell Death Induction *J. Med. Chem.* **2015**, *58*, 1736-1749.
- (11) Vachova, L.; Machacek, M.; Kucera, R.; Demuth, J.; Cermak, P.; Kopecky, K.; Miletin, M.; Jedlickova, A.; Simunek, T.; Novakova, V.; Zimcik, P. Heteroatom-substituted tetra(3,4-pyrido)porphyrazines: a stride toward near- infrared-absorbing macrocycles *Org. Biomol. Chem.* **2015**, *13*, 5608-5612.
- (12) Zimcik, P.; Miletin, M.; Radilova, H.; Novakova, V.; Kopecky, K.; Svec, J.; Rudolf, E. Synthesis, Properties and *In Vitro* Photodynamic Activity of Water-soluble Azaphthalocyanines and Azanaphthalocyanines *Photochem. Photobiol.* **2010**, *86*, 168-175.
- (13) Makhseed, S.; Machacek, M.; Alfadly, W.; Tuhl, A.; Vinodh, M.; Simunek, T.; Novakova, V.; Kubat, P.; Rudolf, E.; Zimcik, P. Water-soluble non-aggregating zinc phthalocyanine and in vitro studies for photodynamic therapy *Chem. Commun.* **2013**, *49*, 11149-11151.